Journal of Power Sources 180 (2008) 767–772

Contents lists available at ScienceDirect

Journal of Power Sources

journal homepage: www.elsevier.com/locate/jpowsour

Optimization of structural combinations on the performance of a PEMFC's MEA

Levent Akyalçın, Süleyman Kaytakoğlu*

Department of Chemical Engineering, Anadolu University, İki Eylül Campus, 26555 Eskişehir, Turkey

ARTICLE INFO

Article history:
Received 2 November 2007
Received in revised form 2 February 2008
Accepted 15 February 2008
Available online 10 March 2008

Keywords:
PEMFC
Sputter
Structural combination
Taguchi's method
ANOVA

ABSTRACT

In this study, the Taguchi method was applied to determine optimum structural combination of a membrane electrode assembly (MEA) in obtaining maximum power density of a PEMFC. Performance measure analysis was also followed by performing a variance analysis, in order to determine the optimum levels and relative magnitude of the effect of combinations. The optimum structural combinations of MEA were found to be membrane, Nafion 112 with a thickness of 51 μm, amount of platinum loaded by sputtering, 0.05 mg Pt cm^{-2}, Nafion ionomer content, 0.05 mg cm^{-2} and support material of gas diffusion layer (GDL), carbon paper. Under these conditions, the amount of maximum power density was predicted as 563.75 mW cm^{-2} by using experimental results obtained according to Taguchi's orthogonal array (OA) $L_{16}(2^4 \times 2^2)$. Verification experiment was done for the same optimum structural combination and maximum power density was observed as 566 mW cm^{-2}. According to the results of this optimization, it was seen that amount of platinum loaded by sputtering and thickness of membrane were the effective parameters.

1. Introduction

Proton exchange membrane fuel cell (PEMFC), operating at low temperatures and high power densities, is considered as being one of the most promising technology able to produce efficient and environmentally friendly energy for powering electrical vehicles [1]. The performance of PEMFC, being important and getting more and more attention in recent years, is known to be influenced by structural parameters of membrane electrode assembly (MEA) as well as operating parameters of PEMFC. While temperatures both fuel cell and humidifiers, pressure, flow rates and relative humidity of fuel and oxidant gases are accepted as operating parameters of a PEMFC, thickness of proton exchange membrane, amount of Pt and Nafion ionomer loaded and finally type of support material of gas diffusion layer (GDL) are counted in structural parameters of a MEA. An effective MEA is one that correctly balances the transport the reactants gases from gas channels to the catalyst layer through GDL, protons from anode side catalyst layer through membrane to the cathode side catalyst layer, electrons from the current collector to the catalyst through GDL and the product gases from the catalyst layer through GDL to gas channels. The effects of the operating parameters on the performance of PEMFC have been widely studied and even optimized by using Taguchi method [2]. The structural parameters being not operating variables, i.e. they cannot be modified during the cell utilization, should be optimized before an MEA production [3].

In literature, it can be seen a lot of studies that deal with or discuss separately the structural parameters affecting the performance of MEA and PEMFC as well. Sasikumar et al. examined the correlation of platinum loading and optimum Nafion ionomer content in the electrode and found that optimum Nafion ionomer requirement depends on the platinum loading and it increases with decrease in Pt loading [4]. The effect of the Nafion ionomer content on the electrode polarization of a PEMFC was investigated and found that film thickness changes with Nafion ionomer loading and activity increases up to an ionomer loading of 1.3 mg cm^{-2} [5]. Effects of the hydrophobic polymer content being both anode and cathode gas diffusion layer on the performance of PEMFC was studied and found that a MEA consisting of 10 wt.% PTFE impregnated GDL showed higher power density than those having PTFE up to 40% in all humidification conditions used in this study [6]. In another study comparing the performance of carbon paper and carbon cloth as a support material of GDL showed that carbon paper was superior to the carbon cloth under dry conditions due to its highly tortuous pore structure [7]. The effect of the porosity of the GDL on the performance of PEMFC were studied and found that performance depends not only on porosity but on the thickness and content of the GDL [8]. The proton conductivity of a series of Nafion membranes was studied by using current-interrupt technique and found that conductivity of the membranes decreases with decreas-

* Corresponding author. Tel.: +90 222 3213550x6308; fax: +90 222 3239501.
E-mail address: skaytako@anadolu.edu.tr (S. Kaytakoğlu).

0378-7753/$ – see front matter © 2008 Elsevier B.V. All rights reserved.
doi:10.1016/j.jpowsour.2008.02.036

Nomenclature

e_i	the random error in ith experiment
n	the number of rows in the matrix experiment
n_{A_i}, n_{B_i}, n_{C_i}, ...	the replication number for parameter level A_i, B_i, C_i, ...
nr	the number of repetition for verification experiment or experimental combination
n_0	equivalent sample size
OA	orthogonal array
Se	the two-standard-deviation confidence limit
S/N	performance characteristics for larger-the better
X_i	the fixed effect of the parameter level combination used in ith experiment
Y_i	performance value of ith experiment

Greek letters

μ	the overall mean of performance value
σ_e^2	error variance

ing membrane thickness [9]. Due to high cost of Pt loading obtained by using conventional technique, the development research leading in the same time to the increase of the electrical performance of PEMFC to decrease the Pt loading of MEA by using sputter technique is of great interest in recent fuel cell applications [10–22].

In order to improve fuel cell performances, it is essential to understand these parametric effects on the fuel cell operations and optimize them [23]. The optimization of the components and their amounts affecting the performance of MEA in PEMFC and obtaining related data are very important in various applications, and especially for fuel cell producers to validate and improve their models [23]. Therefore, doing large numbers of experiments are often needed to understand clearly the effects of the parameters on the performance of MEA and to optimize them. It is known very well that performing large numbers of experiments of systematic experimental studies to optimize the component of MEA are costly and time consuming process. To overcome this challenge, Taguchi's OA analysis, known as experimental design methods, may be used in order to evaluate the respective impacts of those parameters on the performance of PEMFC, and to reduce the number of experiments when many parameters are studied. The main advantage of this method over other statistical experimental design methods is that the parameters affecting an experiment can be investigated as controlling and none controlling. Detail about the Taguchi's OA analysis can be found elsewhere [24–27]. The advantage of the Taguchi method on the conventional experimental design methods, in addition to keeping the experimental cost at a minimum level, is that it minimizes the variation in product response while keeping the mean response on target. Its other advantage is that the optimum component combination determined from the laboratory work can also be reproduced in the real application of PEMFC.

In this work, to ensure for the proper and optimal component combination like membrane thickness, amount of Pt catalyst sputtered, presence of Nafion in the catalyst layer and support material of GDL Taguchi's experimental design method has been used. Results obtained both experimentally and theoretically are given and analyzed in this paper.

2. Material and methods

In this study, Nafion 112, 1135, 115 and 117 membranes with thicknesses 51, 89, 127 and 178 μm, respectively, were used as an electrolyte. The 30 wt.% Teflon based GDLs with a thickness around 400 μm (SGL Carbon 10BB carbon paper and Electrochem carbon cloth used as support material) were used as the substrates, the surfaces of which were the target of sputtering. All electrodes had an active surface area 5 cm^2. When it was desired to investigate the effect of ionomer solution, the surface of GDL's for both the anode and cathode were impregnated with 5 wt.% Nafion solution (0.05 mg cm^{-2}) by air brush before sputtering. The sputter-deposition of Pt on gas diffusion layers was carried out in an argon atmosphere at low pressures (0.08 mbar) by Agar Sputter Coater B7340. The amount of platinum deposited on the GDL's was controlled by the deposition time. Amount of Pt loaded as thickness of Pt layer versus time was determined by atomic forced microscopy (AFM) measurements.

Table 1
Parameters and their values corresponding to their levels studied in experiments

Parameters	Levels			
	1	2	3	4
(A) Nafion membrane	112	1135	115	117
(B) Amount of Pt (mg cm^{-2})	0.01	0.03	0.05	0.10
(C) Amount of ionomer (mg cm^{-2})	0	0.05		
(D) Support material of GDL	Carbon cloth	Carbon paper		

A schematic drawing of the experimental apparatus employed in this study is shown in Fig. 1. In each run, pure hydrogen with a flow rate 1.2 times of its theoretical amount and oxygen with a flow rate 2.0 times of its theoretical amount were used as reacting gas in anode and cathode, respectively. Humidification of the reacting gases was maintained externally by using stainless steel bottles placed in a water bath having a temperature of 75 °C. Regulating the water bath temperature controls the humidification of the reactant gases. Humidification of gases was 100%. The gas connection between the gas control system and the fuel cell inlets are well insulated to prevent condensation of the water vapor on the way to the fuel cell. A single PEMFC made of stainless steel type 316 on house with active surface area of 5 cm^2 was used for all run. Fuel cell temperature was kept at 75 °C by two silicon heaters, each 30 W, located at external surfaces of stainless steel fuel cell separately. This active area was obtained by grooving gas channels having 1 mm depth and 1 mm width in serpentine shape flow field on the center of the each stainless steel 316 end plates. In this study, a fuel cell test station made on house is used. This station includes a computer-based control and data acquisition system through a computer equipped with Labview®-based application software. In this test station, fuel cell and water bath temperatures are controlled by METER EVO 04, which is a microprocessor-based temperature/process controller. Control of flow rates of the reacting gases were maintained via Brooks mass flow controllers located before the humidifiers. Pressures of the anode and cathode sides are controlled at 4 bar by Brooks back pressure regulators. The mass flow rates of reacting gases are set and read through the software. The fuel cell polarization curves are obtained from this program as well by controlling the Agilent N3304 Electronic Load, which measures the voltage versus current response of the fuel cell.

Experimental parameters and their levels given in Table 1 are determined in the light of literature and preliminary tests. The OA experimental design was accepted as the most proper method to determine the experimental plan, $L_{16}(2^4 \times 2^2)$, for four parameters of two of these has four values and two of these has two values given in Table 2 [24–27]. The performance of MEA can be affected by some factors known as controllable or uncontrollable (noise sources). In order to observe the effects of uncontrollable factors on this MEA, each experiment was repeated two times with same conditions. Performance characteristics selected to be the optimization cri-

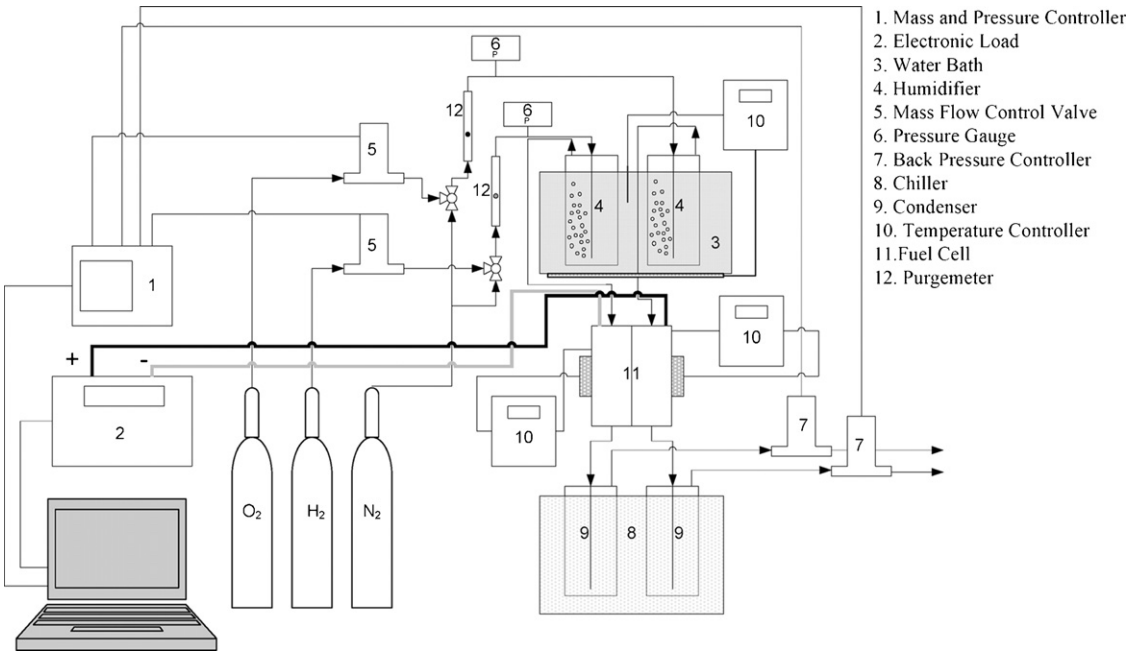

Fig. 1. Schematic representation of experimental apparatus.

teria are divided into three categories, the larger-the-better, the smaller-the-better and the nominal-the-best. The first of them was calculated by using Eq. (1) [26].

$$\text{larger-the-better}: \quad \frac{S}{N} = -10\log_{10}\left(\frac{1}{n_r}\sum_{i=1}^{n_r}\frac{1}{Y_i^2}\right) \tag{1}$$

The values that make S/N maximum are optimum if the purpose of a process is to reach the maximum power density value. The experiment corresponding to optimum working conditions in obtaining the maximum power density might not be found in planned experimental plan table of the Taguchi method. In such cases, the performance value for optimum conditions in obtaining the maximum power density can be predicted by using the balanced characteristic of OA. For this purpose, an additive model given below can be used [27]:

$$Y_i = \mu + X_i + e_i \tag{2}$$

Since Eq. (2) is point estimation, which is calculated by using experimental data in order to determine whether the additive model is adequate or not, the confidence limits for the prediction error must be evaluated [28]. The prediction error is the difference between the observed Y_i and the predicted Y_i. The confidence limits for the prediction error, Se, is

$$\text{Se} = \pm 2\sqrt{\frac{1}{n_o}\sigma_e^2 + \frac{1}{n_r}\sigma_e^2} \tag{3}$$

$$\sigma_e^2 = \frac{\text{sum of squares due to error}}{\text{degrees of freedom for error}} \tag{4}$$

$$\frac{1}{n_o} = \frac{1}{n} + \left[\frac{1}{n_{A_i}} - \frac{1}{n}\right] + \left[\frac{1}{n_{B_i}} - \frac{1}{n}\right] + \left[\frac{1}{n_{C_i}} - \frac{1}{n}\right] + \cdots \tag{5}$$

If the prediction error is outside of these limits, it is ought to be suspected of the possibility that the additive model is not convenient. Otherwise, it can be considered that the additive model is convenient.

A verification experiment is a powerful tool for investigating the presence of interactions among the control parameters. If the predicted response under the optimum conditions in obtaining the maximum power density does not match the observed response, then it implies that the interactions are important. If the predicted response matches the observed response, then it implies that the interactions are probably not important and that the additive model is a good approximation [27]. In the present work, the order of the experiments was obtained by inserting parameters into the columns of OA, $L_{16}(2^4 \times 2^2)$, selected to be the experimental plan given in Table 2. The order of experiments randomized in order to avoid noise sources which had not been considered initially and which could take place during an experiment and affect results in a negative way.

Table 2
Experimental plan table according to L_{16} $(2^4 \times 2^2)$

Experiment number	A	B	C	D
1	1	1	1	1
2	1	2	1	1
3	1	3	2	2
4	1	4	2	2
5	2	1	1	2
6	2	2	1	2
7	2	3	2	1
8	2	4	2	1
9	3	1	2	1
10	3	2	2	1
11	3	3	1	2
12	3	4	1	2
13	4	1	2	2
14	4	2	2	2
15	4	3	1	1
16	4	4	1	1

3. Results and discussion

3.1. Polarization and power density curves

Order of the experiments, in Table 2, were randomized and then performed by using the experimental set-up given in Section 2. Since system conditioning took approximately two hours,

Table 3
Results obtained at cell potential of 0.4 V for the conditions given in Table 2

Experiment number	Current (mA)		Power density (mW cm^{-2})		Average power density (mW cm^{-2})
1	4763	4400	381	352	367
2	3375	3200	270	256	263
3	7375	6775	590	542	566
4	7500	7250	600	580	590
5	4363	3763	349	301	325
6	4575	4375	366	350	358
7	5213	5350	417	428	423
8	5788	5600	463	448	456
9	3538	3863	283	309	296
10	4238	4275	339	342	341
11	5300	5363	424	429	427
12	5075	4763	406	381	394
13	3163	3325	253	266	260
14	4525	4625	362	370	366
15	4488	4650	359	372	366
16	4300	4250	344	340	342

polarization scans were started thereafter. In each run, performed galvanostatically, the polarization scans were taken six times under same working conditions for each MEA. Experiments were repeated two times for every MEA combination prepared different times. Maximum power density was obtained at 0.4 V at each run. Results, consisting of average of the maximum power densities, were presented in Fig. 2 as potential versus current density and power density versus current density curves. Maximum power densities obtained from results were tabulated in Table 3.

3.2. Statistical analysis

The Minitab14® software was used to analyze the collected data. A variance analysis was performed in order to see effective MEA parameters and their confidence levels in obtaining the maximum power density of PEMFC. A statistical analysis of variance (ANOVA) was performed to understand whether the MEA parameters are statistically significant or not. *F*-test is a powerful tool to observe which MEA parameters have a significant effect in obtaining the maximum power density. The *F*-value for each MEA parameter is simply a ratio of the mean of the squared deviations to the mean of squared error. Generally, the larger the *F*-value, the greater the effect on obtaining the maximum power density because of change of the parameter is. The optimal combination of MEA parameters can be predicted together with the performance characteristics and ANOVA analyses. The results of variance analysis for the experiments are given in Table 4.

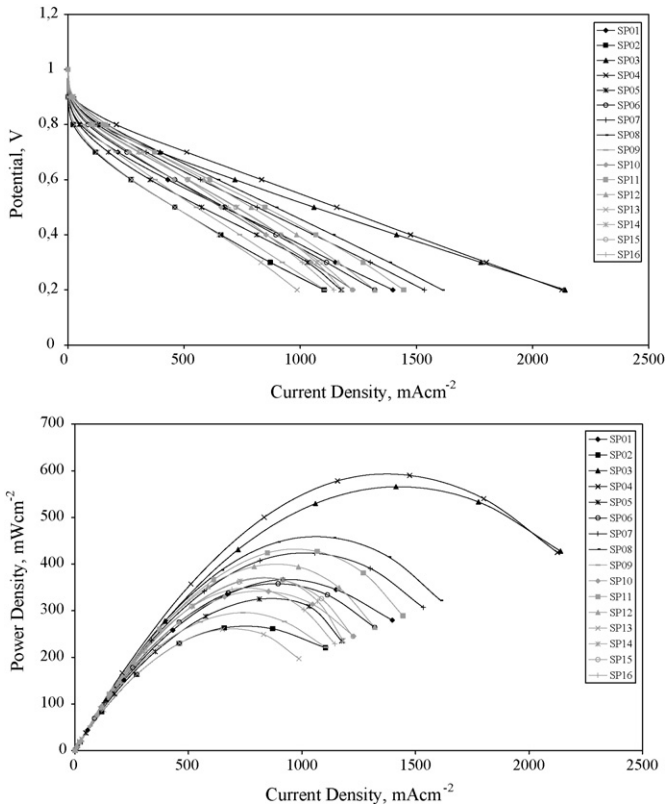

Fig. 2. Polarization and power density curves recorded for the conditions given in Table 2.

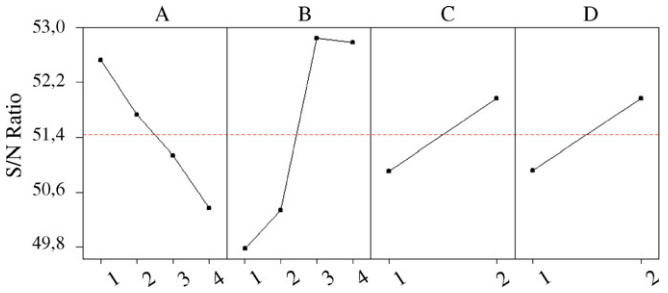

Fig. 3. The mean effects plot for S/N ratios.

The larger the better performance characteristic, Eq. (1), has been taken in obtaining the maximum power density of PEMFC. The order of graphs in Fig. 3 prepared for the experiments is according to the degrees of the influences of parameters on the performance characteristics. The optimal level of a process parameter in obtaining the maximum power density is the level with the highest S/N value calculated by Eq. (1). In Fig. 3A shows the variation of performance characteristics with membrane thickness. In order to determine the experimental conditions for the first data point, A for that point is level 1, which is Nafion 112 membrane for this

Table 4
Result of the variance analysis for the maximum power density value of experiment

	Degree of freedom	Sum of squares	Average of squares	*F*	*p*
A	3	55194	18398	11.25	0.000
B	3	123391	41130	25.14	0.000
C	1	25992	25992	15.89	0.001
D	1	23436	23436	14.33	0.001
Error	23	37622	1636		
Total	31	265636			

Table 5
Optimum MEA combination, and observed and predicted maximum power densities

Parameter	Value	Level
Nafion membrane	112	1
Amount of Pt (mg cm^{-2})	0.05	3
Amount of ionomer (mg cm^{-2})	0.05	2
Support material of GDL	Carbon paper	2
Observed maximum power density (mW cm^{-2})	566	
Predicted maximum power density (mW cm^{-2})	563.75	
Confidence limits of prediction for maximum power density (mW cm^{-2})	438.27–689.24	

parameter. The experiments for which A Level (column A) is 1 are experiments nos. 1–4. The performance characteristics value of the first data point is thus the average of those obtained from experiments numbers 1–4. All the points in Fig. 3A graph and other graphs are obtained by using the same way. The numerical value of the maximum point in each graph is corresponding to the best value for that parameter. These values are seen to be A1 (Nafion 112), B3 (0.05 mg Pt cm^{-2}), C2 (0.05 mg cm^{-2}) and D2 (carbon paper GDL). If the experimental plan given in Table 2 is examined carefully together with parameter values given as maximum power density conditions, it can be seen that experiments corresponding to optimum for maximum power density conditions have been carried out during third experiment conditions.

The results of variance analysis for the experiments are given in Table 4. Thus, it should be noted that the maximum power densities given in Table 5 are predicted results by using Eq. (2) and the observed results obtained from third experiment for the same conditions. The results given in Table 5 are also in between confidence limits of predictions. In order to test the predicted results, verification experiments were carried out at the same working conditions. The fact that the power densities from verification experiments are within the calculated confidence intervals calculated from Eqs. (3)–(5) (see Table 5) shows that the experimental results are within a ±5% error range. This case states that there is a good agreement between the predicted values and experimental values, and the interactive effects between the parameters are indeed negligible. It may be concluded that the additive model is adequate for describing the dependence of the performance of this PEMFC on the various parameters [27].

4. Conclusion

The optimization of the structural parameters of MEA, which is obtained by sputtering Pt onto the GDL, affecting the performance of PEMFC and obtaining related data has crucial importance in various PEMFC applications, and especially for fuel cell producers to reduce the cost of their PEMFC products.

In the present study, Taguchi method has been used to determine the optimum structural combination of MEA to obtain maximum power density of a PEMFC.

The orthogonal array $L_{16}(2^4 \times 2^2)$ technique is described for experimental design as it reduces the number of experiments required to investigate a set of parameters and to minimize time and cost while performing experiments.

Experimental investigations into the parameter effects have allowed determining the optimum configuration of MEA design parameters for maximum power density. Results can be summarized as follows:

- Effective parameters on maximum power density from PEMFC are in order of amount of platinum, thickness of Nafion membrane, presence of Nafion ionomer and support material of GDL.
- Optimum conditions within the selected parameter values are Nafion 112 for membrane, 0.05 mg Pt cm^{-2} for amount of sputter deposited platinum, 0.05 mg cm^{-2} for amount of Nafion ionomer impregnated to the anode and cathode and carbon paper for GDL. Under these conditions, maximum power density was obtained to be 566 mWcm^{-2} from the third experiment.
  - o Nafion 112 (51 μm) is thinnest membrane among the others and gave the best result. Because the ohmic resistance of the Nafion membrane decreases with decreasing membrane thickness and this results in a significantly reduced slope in the pseudolinear region of the cell potential versus current density graphs [9].
  - o As it has been previously presented, MEA with low platinum loading can be manufactured by employing micro system technology processes only such as sputter deposition which allows an ultra-low catalyst loading. The catalyst material is applied to the electrode or membrane surface directly and the three-phase boundary (electrode-catalyst-membrane) is formed in a series of precise deposition processes avoiding any application of solution or ink containing arbitrarily distributed catalyst material, which causes the catalyst to be only in contact with the proton conducting membrane or electrode and many catalyst sites to keep passive. An additional advantage of the thin layer catalyst is that it is active in the immediate neighborhood to both the proton-conducting membrane and electrode. At high cell current densities and gas permeability limitations thick catalyst layers are only active closest to the gas supply, i.e. most distant from the proton-conducting membrane [19]. In this study we obtained Pt loading in the MEA with different amounts indicated in Table 1 by adjusting sputtering time. In case of 0.01 and 0.03 mg Pt cm^{-2} Pt loadings performance of fuel cell was lower compared with 0.05 mg Pt cm^{-2} Pt loading. This was attributed to insufficient platinum deposition and low Pt particle concentration may cause ohmic resistance. In the case of 0.10 mg Pt cm^{-2} Pt loading, performance was lower than 0.05 mg Pt cm^{-2} Pt loading due to relatively low catalyst surface area. Another reason of the lower performance the higher resistance is the limiting of the water transport due to less pores caused thicker catalyst layer.
  - o Ionomer content into catalyst layer has positive effect on PEM fuel cell performance. From the perspective of electrode performance, the cost problem can be tackled in two ways: reduction of catalyst loading and improvement of the catalyst utilization and performance. The underlying concept of reducing catalyst loading is to enhance catalyst utilization in the electrode. It is worthwhile to note that only catalyst in contact with both membrane electrolyte and reaction gas is electrochemically active. This has been demonstrated previously via impregnation of solubilized ionomers like Nafion in the electrode [5]. As it can be seen from the results that ionomer loading into electrode increases ionic conductivity, lowers the resistance to proton migration and causes higher cell performance.
  - o Support material of gas diffusion layer has an important role on performance of PEM fuel cell. Temperature of PEM fuel cells increases with increasing current densities, which causes dehydration of proton conductive membrane. However, under dry conditions, the carbon paper shows better performance due to its more tortuous structure, which prevents the loss of product water to dry gas streams, thus increasing the membrane hydration level and reducing the ohmic loss [7]. As seen from our findings, as a support material carbon paper is better than carbon cloth. This may be explained as follows: carbon cloth has too coarse fiber network, which leads to the active layer entering too deeply in support material and causes high ohmic

resistance due to poor contact with catalyst layer compared to dense carbon paper [29].
- Predicted and obtained maximum power densities are very close to each other. It may be concluded that the additive model is adequate for describing the dependency of obtaining maximum power density on various parameters.
- Since optimum conditions determined by Taguchi method in a laboratory scale PEMFC is reproducible in large scale PEMFC as well, findings of present study may be very useful for PEMFC stack applications.

Acknowledgements

Special thanks go to the Scientific Research Project Commission of the Anadolu University for financial support of the present work under project nos.: 020218, 030244 and 050232 and Prof. Dr. Renate Hiesgen for helping of AFM measurements.

References

[1] B. Wahdame, D. Candusso, J.M. Kauffmann, J. Power Sources 156 (1) (2006) 92–99.
[2] S. Kaytakoğlu, L. Akyalçın, Int. J. Hydrogen Energy 32 (2007) 4418–4423.
[3] M.G. Santarelli, M.F. Torchio, Energy Convers. Manage. 48 (1) (2007) 40–51.
[4] G. Sasikumar, J.W. Ihm, H. Ryu, Electrochim. Acta 50 (2004) 601–605.
[5] S.J. Lee, S. Mukerjee, J. McBreen, Y.W. Rho, Y.T. Kho, T.H. Lee, Electrochim. Acta 43 (24) (1998) 3693–3701.
[6] C. Lim, C.Y. Wang, Electrochim. Acta 49 (2004) 4149–4156.
[7] Y. Wang, C.Y. Wang, K.S. Chen, Electrochim. Acta 52 (2007) 3965–3975.
[8] H.S. Chu, C. Yeh, F. Chen, J. Power Sources 123 (2003) 1–9.
[9] S. Slade, S.A. Campbell, T.R. Ralph, F.C. Walsh, J. Electrochem. Soc. 149 (12) (2002) A1556–A1564.
[10] S. Litster, G. Mclean, J. Power Sources 130 (2004) 61–76.
[11] R. O'Hayre, S.J. Lee, S.W. Cha, F.B. Prinz, J. Power Sources 109 (2002) 483–493.
[12] M.F. Weber, S. Mamiche-Afara, M.J. Dignam, L. Pataki, R.D. Venter, J. Electrochem. Soc. 134 (6) (1987) 1416–1419.
[13] E.A. Ticianelli, C.R. Derouin, S. Srinivasan, J. Electroanal. Chem. 251 (1988) 275–295.
[14] S. Mukerjee, S. Srinivasan, A.J. Appleby, Electrochim. Acta 38 (1993) 1661–1669.
[15] S. Hirano, J. Kim, S. Srinivasan, Electrochim. Acta 42 (1997) 1587–1593.
[16] S.Y. Cha, W.W. Lee, J. Electrochem. Soc. 146 (1999) 4055–4060.
[17] A.T. Haug, R.E. White, J.W. Weidner, W. Huang, S. Shi, T.C. Stoner, N. Rana, J. Electrochem. Soc. 149 (2002) A280–A287.
[18] P. Brault, A. Caillard, A.L. Thomann, J. Mathias, C. Charles, R.W. Boswel, S. Escribano, J. Durand, T. Sauvage, J. Phys. D: Appl. Phys. 37 (2004) 3419–3423.
[19] D. Gruber, N. Ponath, J. Müller, F. Lindstaedt, J. Power Sources 150 (2005) 67–72.
[20] K. Huang, Y. Lai, C. Tsai, J. Power Sources 156 (2006) 224–231.
[21] T. Nakakubo, M. Shibata, K. Yasuda, J. Electrochem. Soc. 152 (2005) A2316–A2322.
[22] C.H. Wan, M.T. Lin, Q.-H. Zhuang, C.-H. Lin, Surf. Coat. Technol. 201 (1–2) (2006) 214–222.
[23] L. Wang, A. Husar, T. Zhou, H. Liu, Int. J. Hydrogen Energy 28 (11) (2003) 1263–1272.
[24] R.K. Roy, Design of Experiments Using the Taguchi Approach, Wiley, New York, 2001.
[25] N. Logothetis, H.P. Wynn, Quality Through Design, Clarendon Press, Oxford, 1989.
[26] J.P. Ross, Taguchi Techniques for Quality Engineering, McGraw-Hill, New York, 1988.
[27] M.S. Phadke, Quality Engineering Using Robust Design, Prentice-Hall, Englewood Cliffs, NJ, 1989.
[28] M.S. Phadke, R.N. Kackar, D.V. Speeney, M.J. Grieco, Bell Syst. Tech. J. 62 (5) (1983) 1273–1309.
[29] L. Passalacqua, F. Lufrano, G. Squadrito, A. Patti, L. Giorgi, Electrochim. Acta 43 (24) (1998) 3665–3673.